CFD ANALYSIS OF CIRCULATING FLUIDIZED BED COMBUSTION

Ravindra Kumar and K.M.Pandey
Department of Mechanical Engineering,
Gurgaon Institute of Technology&Management, Gurgaon, India
National Institute of Technology, Silchar, Assam, India

***Abstract*- In this paper computational analysis of circulating fluidized bed combustion using the fluent software is analysed. This work is concerned about gas–solid two-phase mixtures flowing upwards through the fast beds. The procedures studied are applicable to all types of fluidized-bed boilers. The type of information resulting from various ways of analyzing the pressure and temperature in fluidized beds are discussed.**
This paper presents coal combustion in circulating fluidized bed and the k–ϵ two-phase turbulence model was used to describe the gas–solids flow in a CFB. The analysis of coal combustion is done by discrete phase model (DPM) and non pre mixed combustion in species model .Predicting the performance of large scale circulating fluidized bed boilers requires reliable and efficient modeling tools. In a CFB furnace, the fuel, air, and other input materials are fed locally and the mixing of different reactants is limited. The particle size has taken 5 mm and fluidizing velocity (4-6) m/s. As a result of analysis, the variation in mean particle diameter and superficial velocity, does affect the temperature, pressure and turbulence kinetic energy in different mean fractions in the combustion zone. The average temperature is found around the1370k.

***Keywords*- Coal, fluidized bed combustion, Two-phase flow, DPM.**

I. INTRODUCTION

'Getting rid of waste' was the ultimate goal when the fluidized bed combustion (FBC) technology was introduced [1]. This goal evolved over time to 'clean energy for the future'. Since its introduction in the 1970s the technology has gained acceptance in various industrial applications. FBC is a combustion technology used in power plants. FBC is known for its ability to burn low-grade fuels with low calorific value, high ash content and high moisture content. Fluidized beds suspend solid fuels on upward-blowing jets of air during the combustion process. The result is a turbulent mixing of gas and solids. When a fluidized bed is operated above the terminal velocity of the particles, they are carried out of the bed. The system of a circulating fluidized bed (CFB) occurs when the particles are separated from the fluid by the use of cyclones and are recycled to the bed. The part of the system where the carryover of solids transpires is normally referred to as the riser. It is known for its ability to burn low-grade fuels with low calorific value, high ash content and high moisture content. The fluidization process begins when a bed of inert material (usually sand), which is a solid granular particle, is suspended by a flow of air or gas (air). This flow is injected into the combustion chamber from the bottom and from the side. FBC boilers can burn fuels other than coal, and the lower temperatures of combustion (800 °C / 1500 °F) have other added benefits as well.

In this paper, the gas (air) and solid (coal) is injected at the base with different velocities while taking coal particles of different diameters as solid bed. In the 2D CFB combustor have the 3 inlet points such as inlet for fluidizing velocity (primary air), inlet for coal particles and inlet for secondary air. The primary air is used for the fluidized of coal particle and secondary air for proper combustion in the combustor. The combustion processes is done by the discrete phase model and use the single injection system for burning of coal in the combustor.

II. LITERATURE REVIEW

A.Williams and M. Pourkashanian [2] worked on the some of the key issues currently being debated regarding the combustion of coal and of some biomass materials. It attempts to summarize the present approaches toward the quantification of the fundamental processes of solid fuel combustion for use in computer models. Some aspects of the various chemical and physical processes are included, such as heating-up of particles, devolatilization, and subsequent char formation. Of particular interest is the prediction of char properties, such as composition, surface areas, and morphology, since these impacts on char combustion.

Konstantin P. Filipov [3] presented on Mathematical model describing two-phase flow in CFB in framework of external model ash was elaborated. It takes into account the all main processes in high-velocity fluidized bed including processes of the coal combustion and the attrition of ash. On base of this model was developed numerical code and carried out some calculations of transient and stationary performances of CFB. Z.Guangbo [4] focused on a steady state model of a coal-fired circulating fluidized-bed boiler, based on hydrodynamics, heat transfer and combustion, is presented. This model predicts the flue gas temperature, the chemical gas species (O_2, H_2O, CO, CO_2 and SO_2) and char concentration distributions in both the axial and radial locations along the furnace including the bottom and upper portion. The model was validated against experimental data

generated in a 35 t/h commercial boiler with low circulation ratio.

Afsin Gungor [5] worked on a dynamic two dimensional model is developed considering the hydrodynamic behavior of CFB. In the modeling, the CFB riser is analyzed in two regions: The bottom zone in turbulent fluidization regime is modeled in detail as two-phase flow which is subdivided into a solid-free bubble phase and a solid-laden emulsion phase. In the upper zone core–annulus solids flow structure is established. Simulation model takes into account the axial and radial distribution of voidage, velocity and pressure drop for gas and solid phase, and solids volume fraction and particle size distribution for solid phase. The model results are compared with and validated against atmospheric cold bed CFB units' experimental data given in the literature.Hideya Nakamura [6] presented on modeling of particle fluidization behaviors in a rotating fluidized bed (RFB) was conducted. The proposed numerical model was based on a DEM (Discrete Element Method)-CFD (Computational Fluid Dynamics) coupling model. Fluid motion was calculated two dimensionally by solving the local averaged basic equations. Particle motion was calculated two-dimensionally by the DEM. Calculation of fluid motion by the CFD and particle motions by the DEM were simultaneously conducted in the present model. Geldart group B particles (diameter and particle density were 0.5 mm and 918 kg/m3, respectively) were used for both calculation and experiment. Aboozar Hadavand [7] presented on a mathematical model of the circulating fluidized bed combustion system based on mass and energy conservation equations were successfully extracted. Using these correlations, a state space dynamical model oriented to bed temperature has been obtained based on subspace method. Bed temperature, which influences boiler overall efficiency and the rate of pollutants emission, is one of the most significant parameters in the operation of these types of systems. Having dynamic and parametric uncertainties in the model, a robust control algorithm based on linear matrix inequalities (LMI) have been applied to control the bed temperature by input parameters, i.e. coal feed rate and fluidization velocity. Circulating fluidized bed (CFB) combustion systems are increasingly used as superior coal burning systems in power generation due to their higher efficiency and lower emissions.

L.X. Kong and P.D. Hodgson [8] worked on To improve the understanding of the heat transfer mechanism and to find a reliable and simple heat-transfer model, the gas flow and heat transfer between fluidized beds and the surfaces of an immersed object is numerically simulated based on a double particle-layer and porous medium model. The velocity field and temperature distribution of the gas and particles are analyzed during the heat transfer process. The double particle-layer and porous medium model has the ability to simulate the gas flow and the heat transfer near the surface of an immersed object in fluidized beds, and was successfully used in calculating the dynamic characteristics of the gas phase, the temperature change of particles and the radiative parameters of a particle group. The results provide sufficient information to improve the understanding of heat transfer processes near the immersed surface. J.C.S.C. Bastos focused on [9] Radial solids velocity profiles were computed on seven axial levels in the riser of a high-flux circulating fluidized bed (HFCFB) using a two-phase 3-D computational fluid dynamics model. The computed solids velocities were compared with experimental data on a riser with an internal diameter of 76 mm and a height of 10 m, at a high solids flux of $300 kgm^{-2}s^{-1}$ and a superficial velocity of $8ms^{-1}$. Several hundreds of experimental and numerical studies on CFBs have been carried out at low fluxes of less than $200 kgm^{-2}s^{-1}$, whereas only a few limited useful studies have dealt with high solids flux.

A three-dimensional model of a circulating fluidized bed gasifier was developed by [10] I. Petersen and J.Werther, which uses continuous radial profiles of velocities and solids hold-up with regard to the description of fluid mechanics. A complex reaction network of sewage sludge gasification is included in the model. In the simulation calculations the influence of the axial location and the number of feeding points was examined for gasifiers of different scales. It was found that due to the very fast decomposition of the volatiles and the high volatile content in the sewage sludge, lateral mixing of the gas around the feeding port is not complete, and plumes with high pyrolysis gas concentrations are formed. Vidyasagar Shilapuram [11] worked on Experiments were conducted in a liquid–solid circulating fluidized bed (LSCFB) to study the flow regimes, operational instability, critical transitional velocity to circulating fluidized bed (CFB) regime, solids holdup and solids circulation rate by three experimental methods. The results indicate that the operational instabilities such as arch formation, liquid–solid separator blockage and solids return pipe blockage were observed in two of these methods at large primary and auxiliary liquid velocities. The critical transitional velocity that demarcates the expanded bed from CFB regime was observed to be different by these three methods. The macroscopic flow properties (flow regimes, onset of average solids holdup, average solids holdup and solids circulation rate in the riser) are different by different methods of operation.Jack T. Cornelissen [12] discussed on a multiplied Eulerian computational fluid dynamics (CFD) model with granular flow extension is used to simulate a liquid–solid fluidized bed. The numerical simulations are evaluated qualitatively by experimental data from the literature and quantitatively by comparison with new experimental data. The effects of mesh size, time step and convergence criteria are investigated. The Eulerian CFD simulations based on FLUENT software for water fluidization of glass spheres give results which are generally in good qualitative and reasonable quantitative agreement with experimental results. Courant number between 0.03 and 0.3 gave good predictions in this work.

Xiao-Bo Qi [13] presented on Friction between co-current down flow gas–solid flow and column wall was investigated by measuring apparent and actual solids concentrations in a circulating fluidized bed (CFB) downer. A new model to predict pressure drops due to friction between the gas–solid suspension in the fully developed zone and the downer wall was developed. The results show that the friction between the gas–solid suspension and the downer wall causes a significant deviation of the apparent solids concentrations from the actual ones, especially for those operating conditions with higher superficial gas velocities and solids circulation rates. When the superficial gas velocity is greater than 8 m/s, the actual solids concentrations in the fully developed region of the downer can be up to two to three times of the apparent values. Particle diameters have different influences on the frictional pressure drops under different superficial gas velocity.

Haiyan Zhu [14] focused on detailed local flow structures are investigated in bubbling and turbulent fluidized bed with FCC particles. The operating conditions ranges from 0.06 to 1.4 m/s. Extensive experiments are carried out using a newly developed optical fiber probe system, which can measure the solids concentration and velocity at multi-points. The results reveal that with increasing Ug, local solids concentrations go through three evolution stages, reflecting a gradual regime transition process. Under all operating conditions, up flowing and descending particles co-exist at all measuring locations. Results show that in the turbulent fluidized bed a stable two-phase flow structure breaks down and the solids concentration and velocity distribution is not at all uniform in both radial and axial directions. Zhongxiang Chen [15] described on the performance of fluidized bed methane reformers with three models—a simple equilibrium model and two kinetic distributed models, based on different assumptions of varying sophistication. Membranes are incorporated to improve reactor performance. Eighteen cases are simulated for different flow regimes and membrane configurations. Predictions for the fast fluidization and turbulent flow regimes show that the rate-controlling step is permeation through the membranes. Bubbling regime simulations predict somewhat less hydrogen production than for turbulent and fast fluidization, due to the effects of interphase crossflow and mass transfer.

Stephen J. Goidich [16] focused on Circulating fluidized bed technology has moved into the utility power generation market with units as large as 250 MWe in operation, two (2) 300 MWe units in the construction phase, and designs developed for units as large as 600 MWe in size. Technology improvements are continually being developed and incorporated in the designs to enhance performance, increase operational flexibility, and improve reliability in a cost-effective way. Most notable is the Compact CFB boiler with INTREXTM heat exchanger which Foster Wheeler introduced in the early 1990's.Adnan Almuttahar [17] performed on CFD modeling of air and fluid catalytic cracking (FCC) particles in the riser of a high density circulating fluidized bed (HDCFB). The implementation of correct inlet conditions was found to be critical for the successful simulation of the hydrodynamics. The simulated profiles of gas and solid velocity and volume fraction were overall in good agreement with experimental data reported in the literature. However, due to the difficulties in accurate modeling of the solid segregation toward the wall, the solid volume fraction was under predicted near the walls. The effect of modeling parameters including different drag models, wall restitution coefficient values, and solid slip conditions have been evaluated.

Ernst-Ulrich Hartge [18] presented on a model of the fluid mechanics in the riser of a circulating fluidized bed (CFB) has been implemented using computational fluid dynamics (CFD). The model developed shall be used in future as the basis of 3D-reactor model for the simulation of large scale CFB combustors. The two-fluid model (TFM) approach is used to represent the fluid mechanics involved in the flow. The computational implementation is accomplished by the commercial software FLUENT. As result of this study, a formulation is established from the variety of available models. As a major finding of this part it has been shown, that the commonly used drag correlations with an increasing drag with increasing solids concentration fail to predict a dense bottom zone in the CFB riser, as is observed in reality. Taking the sub-grid heterogeneity of the flow into account, as is done here with the help of the EMMS model, allows predicting the dense bottom zone.

Xiao-Bo Qi and Hui Zhang [19] worked on the investigate solids concentration in the fully developed region of co-current downward gas–solid flow, actual solids concentrations were measured in a circulating fluidized bed (CFB) downer with 9.3 m in height and 0.1 m in diameter using a fiber optical probe. The results obtained from this work and in the literature show that the average solids concentration in the fully developed region of the CFB downers is not only a function of the corresponding terminal solids concentration, but the operating conditions and particle properties also have influences on the average solids concentration in the fully developed region of the CFB downers. Jinsen Gao and Jian Chang [20] presented on the experimental and computational studies on the flow behavior of a gas–solid fluidized bed with disparately sized binary particle mixtures. The mixing/segregation behavior and segregation efficiency of the small and large particles are investigated experimentally. Particle composition and operating conditions that influence the fluidization behavior of mixing/segregation are examined. Based on the granular kinetics theory, a multi-fluid CFD model has been developed and verified against the experimental results. The simulation results are in reasonable agreement with experimental data. The results showed that the smaller particles are found near the bed surface while the larger particles tend to settle down to the bed bottom in turbulent fluidized bed. Ernst-Ulrich Hartge [21] invented on a model

of the fluid mechanics in the riser of a circulating fluidized bed (CFB) has been implemented using computational fluid dynamics (CFD). The model developed shall be used in future as the basis of 3D-reactor model for the simulation of large scale CFB combustors. The two-fluid model (TFM) approach is used to represent the fluid mechanics involved in the flow. The computational implementation is accomplished by the commercial software FLUENT. Different closure formulations are tested on a simplified geometry. The work presented here consists of two major parts. The first part involves a formulation study, where several combinations of granular temperature formulation, turbulence models, approaches to solids phase turbulence, drag correlations and solid–solid restitution coefficients are tested. Macroscopic (semi-empirical) models for fluid dynamics of circulating fluidized bed (CFB) units are presented [22] by Filip Johnsson, with emphasize on applications for conditions relevant to industrial units such as fluidized-bed combustors. In order to make a structured analysis of the models, the CFB unit is divided into 6 fluid dynamical zones, which have been shown to exhibit different fluid-dynamical behaviour (bottom bed, freeboard, exit zone, exit duct, cyclone and downcomer and particle seal). The paper summarizes the main basis and assumptions for each model together with major advantages and drawbacks. Dongsheng wen and Yurong He [23] developed on gas–solid two-phase mixtures flowing upwards through packed beds. An Eulerian-based two-fluid model coupled with a newly proposed porosity distribution model is used to simulate the flow behaviour. The results are compared with recently published experimental results in terms of both hydrodynamics and solids motion. It is found that the use of the newly proposed porosity model not only gives better agreement with experimental porosity data, but also provides a much better prediction of the pressure drop than other porosity models could do. The results also show that the model predicts very well the dynamic hold-up of suspended particles, and captures the main features of the radial distributions of the suspended solids concentration and the axial solids velocity.Peng Li [24] performed on the suitability of various drag models for predicting the hydrodynamics of the turbulent fluidization of FCC particles on the Fluent V6.2 platform. The drag models included those of Syamlal–O'Brien, Gidaspow, modified Syamlal–O'Brien, and McKeen. Comparison between experimental data and simulated results showed that the Syamlal–O'Brien, Gidaspow, and modified Syamlal–O'Brien drag models highly overestimated gas–solid momentum exchange and could not predict the formation of dense phase in the fluidized bed, while the McKeen drag model could not capture the dilute characteristics due to underestimation of drag force. The standard Gidaspow drag model was then modified by adopting the effective particle cluster diameter to account for particle clusters, which was, however, proved inapplicable for FCC particle turbulent fluidization. The simulated results showed that they all failed due to either underestimation or overestimation of the drag force between the gas and the solid phase.

III. GOVERNING EQUATIONS OF FLUID DYNAMICS

III.I CONTINUITY EQUATION

The conservation of mass equation or continuity equation [28] is given by

$$\frac{\partial \rho}{\partial t} + \nabla.\left(\rho \vec{V}\right) = 0 \qquad (3.1)$$

Where ρ is the density, $\vec{V}$ is the velocity vector.

III.II MOMENTUM EQUATION

Applying the Newton's second law $(force = mass \times acceleration)$ the conservation of momentum equation is given by

$$\frac{\partial}{\partial t}\left(\rho \vec{V}\right) + \nabla.\left(\rho \vec{V}\,\vec{V}\right) = -\nabla p + \nabla.\bar{\bar{\tau}} + \rho\vec{g} + \vec{F} \qquad (3.2)$$

Where ρ is the density, $\vec{V}$ is the velocity vector, p is the static pressure, and $\bar{\bar{\tau}}$ is the stress tensor (described below), and $\rho\vec{g}$ and $\vec{F}$ are the gravitational body force and external body forces (e.g., that arise from interaction with the dispersed phase), respectively. The stress tensor $\bar{\bar{\tau}}$ is given by

$$\bar{\bar{\tau}} = \mu\left[\left(\nabla.\vec{V} + \nabla.\vec{V}^{T}\right) - \frac{2}{3}\nabla.\vec{V}I\right] \qquad (3.3)$$

Where μ is the molecular viscosity, I is the unit tensor, and the second term on the right hand side is the effect of volume dilation.

III.III ENERGY EQUATION

Energy is neither created nor destroyed. It is always conserved. The conservation of energy equation is given by

$$\frac{\partial}{\partial x}(\rho E) + \nabla.\left(\vec{v}(\rho E + p)\right) = \nabla.\left(k_{eff}\nabla T - \sum_{j} h_j \vec{J}_j + \left(\bar{\bar{\tau}}_{eff}.\vec{v}\right)\right) + S_h$$

(3.4)

$$E = h - \frac{p}{\rho} + \frac{v^2}{2} \qquad (3.5)$$

where sensible enthalpy h is defined for ideal gaseas

$$h = \sum_{j} Y_j h_j$$

(3.6) For incompressible flows as

$$h = \sum_j Y_j h_j + \frac{p}{\rho} \quad (3.7)$$

These equations form a set of coupled, nonlinear partial differential equations. It is not possible to solve these equations analytically for most engineering problems. However, it is possible to obtain approximate computer-based solutions to the governing equations for a variety of engineering problems. This is the subject matter of Computational Fluid Dynamics (CFD).

III.IV ENERGY EQUATION FOR NON-PREMIXED COMBUSTION MODEL

When the non-adiabatic non-premixed combustion model is enabled, FLUENT solves the total enthalpy form of the energy equation

$$\frac{\partial}{\partial t}(\rho H) + \nabla.(\vec{v}H\rho) = \nabla.\left(\frac{k_t}{c_p}\nabla H\right) + S_h \quad (3.8)$$

Under the assumption that the Lewis number (Le) = 1, the conduction and species diffusion terms combine to give the first term on the right-hand side of the above equation while the contribution from viscous dissipation appears in the non-conservative form as the second term. The total enthalpy $\mathbf{H}$ is defined as

$$\mathbf{H} = \sum_j \mathbf{Y_j H_j} \quad (3.9)$$

Where $\mathbf{Y_j}$ is the mass fraction of species $\mathbf{j}$ and

$$\mathbf{H_j} = \int_{T_{ref,j}}^{T} \mathbf{c_{pj}} dT + \mathbf{h_j^0(T_{ref,j})} \quad (3.10)$$

$\mathbf{h_j^0(T_{ref,j})}$ is the formation enthalpy of species $\mathbf{j}$ at the reference temperature $\mathbf{T_{ref,j}}$.

IV. STANDARD K - Є MODEL

The turbulence models are the two-equation models. The simplest one is the standard *k* - *ϵ* model, which is proposed by *Launder and Spalding*. It is widely used in turbulence simulations because of its general applicability, robustness and economy. The two transport equations for the kinetic energy and dissipation rate are solved to form a characteristic scale for both turbulent velocity and length. These scales represent the turbulent viscosity.

The modeled transport equations for K and Є in the realizable K - Є model are

$$\frac{\partial}{\partial t}(\rho k) + \frac{\partial}{\partial x_j}(\rho k u_j) = \frac{\partial}{\partial x_j}\left[\left(\mu + \frac{\mu_t}{\sigma_k}\right)\frac{\partial k}{\partial x_j}\right] + G_k + G_b - \rho\varepsilon - Y_M \quad (4.1)$$

$$\frac{\partial}{\partial t}(\rho\varepsilon) + \frac{\partial}{\partial x_j}(\rho\varepsilon u_j) = \frac{\partial}{\partial x_j}\left[\left(\mu + \frac{\mu_t}{\sigma_\varepsilon}\right)\frac{\partial \varepsilon}{\partial x_j}\right] + \rho C_1 S_\varepsilon - \rho C_2 \frac{\varepsilon^2}{k + \sqrt{\varepsilon v}} + C_{1\varepsilon}\frac{\varepsilon}{k}C_{3\varepsilon}G_b + S_\varepsilon \quad (4.2)$$

$$C_1 = max\left[0.43, \frac{\eta}{\eta + 5}\right], \quad \eta = S\frac{k}{\varepsilon}, S = \sqrt{2S_{ij}S_{ij}}$$

In these equations, G_k represents the generation of turbulence kinetic energy due to the mean velocity gradients. G_b is the generation of turbulence kinetic energy due to buoyancy. Y_M represents the contribution of the fluctuating dilatation in compressible turbulence to the overall dissipation rate. C_2 and C_{1C} are constants. σ_k and σ_C are the turbulent Prandtl numbers for K and Є respectively. S_k and S_C are user-defined source terms.

V. CFD MODEL OF FLUIDIZED BED

The furnace model considered for analysis of coal combustion is 15m height and 3.2 m diameter of the lower part of the furnace. The purpose of the work was to study the char at the lower part of the furnace. The model volume was restricted to a 15 m height section of the furnace [28].Model geometry in two-dimensional and three-dimensional as shown in fig. 6.2.Circulating bed is fluidized by primary air through the grid. Secondary air is introduced at level 2 – 4 m from grid. From the furnace, the gas and solids enter the separator, which separates the solids from flue gas. A circulating fluidized bed is one where fuel is burnt in a fast fluidized bed regime. In CFB boiler furnace the gas velocity is sufficiently high to blow all the solids out of the furnace.

The majority of solids leaving the furnace is captured by gas-solid separators.

VI. COMPUTATION GRID GENERATION

VI.I MODEL CREATION AND GRID GENERATION IN GAMBIT

For the furnace as explained in a two dimensional model is created in GAMBIT 2.3.16. The 2D view of the furnace after modeling is as shown in Fig.1.

VI.II GRIDS SELECTED FOR THE PRESENT WORK

The grids are selected for all the meshes for doing CFD analysis. As the furnace for which analysis is carried out, quadrate type mesh is selected. This specifies that the mesh is composed primarily of quadrate mesh elements. The qualities of the created mesh are checked.

Fig.1. View of the model in 2D after modeling in GAMBIT 2.3.16

GAMBIT 2.3.16 was used for making 2D furnace geometry with width of 3.2m from the lower part and height 15m. Coarse mesh size of 0.01m was taken in order to have 9365 cells (18952 faces) and 9588 nodes for the whole geometry. It was used in order to have better accuracy. But using mesh results in 9365 cells (18952 faces), which requires smaller time steps, more number of iterations per time step and 4 times more calculation per iteration for the solution to converge. The model of combustion chamber with boundary conditions as below.

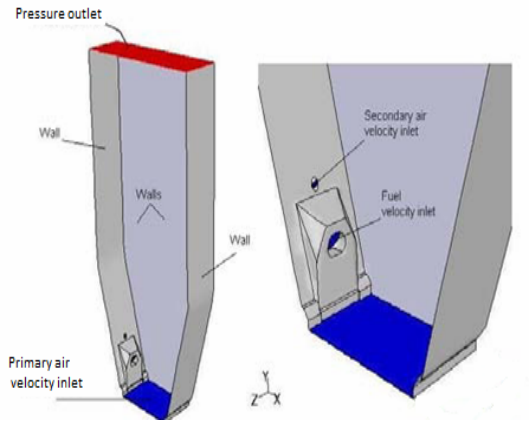

Fig.2. Combustion chamber in 3D

VII. DISCRETE PHASE MODEL (DPM)

In addition to solving transport equations for the continuous phase, FLUENT allows you to simulate a discrete second phase in a Lagrangian frame of reference. This second phase consists of spherical particles (which may be taken to represent droplets or bubbles) dispersed in the continuous phase. FLUENT computes the trajectories of these discrete phase entities, as well as heat and mass transfer to/from them. The coupling between the phases and its impact on both the discrete phase trajectories and the continuous phase flow can be included.

FLUENT provides the following discrete phase modeling options:

1) Calculation of the discrete phase trajectory using a Lagrangian formulation that includes the discrete phase inertia, hydrodynamic drag, and the force of gravity, for both steady and unsteady flows
2) Combusting particles, including volatile evolution and char combustion to simulate coal combustion
3) These modeling capabilities allow FLUENT to simulate a wide range of discrete phase problems including particle separation and classification, spray drying, aerosol dispersion, and bubble stirring of liquids, liquid fuel combustion and coal combustion.

VIII. PROBLEM DESCRIPTION

The problem consists of a two phase fluidized bed in which gas and solid (coal) enters at the separate portion of the domain. For a 2D CFB furnace, estimate the primary air is flowing at 503 k and 4m/s which is flowing through the nozzles .The secondary air is injected at the level of 2.3 m from the level of the bottom at 473 k and 2m/s and the fuel feed rate 0.5 kg/s is injected at the level of 1.5m from the level of the bottom, corresponding to very fuel-lean conditions in the flow. The bed cross-section is 3.2 m x15 m below and 6.7 m x15 m above this level. The Reynolds number, based on inlet conditions and the flow is turbulent. The combustion is modelled using the mixture-fraction approach. The bed consists of solid material (coal particles) of uniform diameter and the size of solid particles is 5000 μm.

Data for coal analysis is given below.

Coal – Lignite (composition on dry) basis

C – 67%, H – 6%, O– 25%, N – 1%, S – 1%, HHV – 25MJ/Kg

IX. ANALYSIS PARAMETERS

Table I:

Parameter	**Value**
Primary air velocity	4-6m/s
Secondary air velocity	2m/s
Coal particle size	5000 μm
Primary air temperature	503k
Secondary air temperature	473k
Mass flow rate	0.5kg/s
Oxygen concentration at inlet	21%
Back flow temperature	1800k
Initial pressure	$1.0.10^5$pa

Coal heat capacity	1000J/kg-k
Coal density	1350kg/m^3
Mean mixture fraction	0.09
Oxide in PDF table	600k

X. SELECTION OF MODELS FOR ANALYSIS

FLUENT 6.2.16 was used for analysis. 2D segregated 1st order implicit steady solver is used. (The segregated solver must be used for multiphase calculations). Standard k-ε model with standard wall functions were used.
The model constants are tabulated as:
Table II:Model constants used for analysis as given below

Cmu	0.09
C1-Epsilon	1.44
C2-Epsilon	1.92
C3-Epsilon	1.3
TKE Prandtl Number	1
TDR Prandtl Number	1.3
Energy Prandtl Number	0.85

The non premixed combustion model is used for combustion and in DPM (discrete phase model) single type injection system is used for the solid fuel combustion.

XI. SOLUTION

The finite volume method was applied to discretize the governing equations on computational grids. Under relaxation factor for pressure, momentum and mixture fraction were taken. The discretization scheme for momentum, mixture fraction, turbulence kinetic energy and turbulence dissipation rate were all first order upwind. Pressure-velocity coupling scheme was Phase Coupled SIMPLE. The solution was initialized from all zones. Iterations were carried out for time step size of 0.01-0.001 depending on ease of convergence and time required to get the result for fluidization. Convergence and accuracy is important during solution. This can be seen by the residual plots in fig.3. If not then we have to change the solution parameters and sometimes solution method also. Currently, K-epsilon method is used for the combustion study of the fluidized bed.

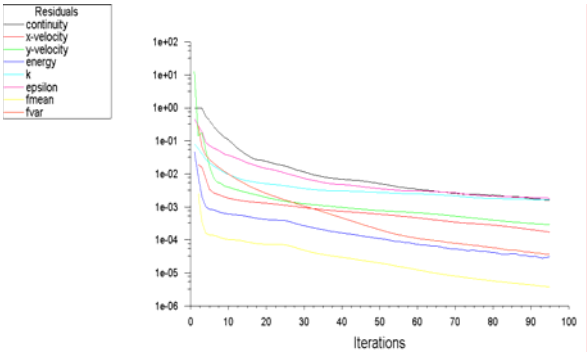

Fig.3. Plot of residuals for k-epsilon solver method as the iterations proceeds.

XII. BOUNDARY CONDITIONS

The boundary conditions are as equally important as the selection of the proper mathematical model. Initially, solid particle velocity was set at in minimum fluidization and gas velocity was assumed to have the same value everywhere in the bed. The temperature of the primary and secondary air was also set to 503k and 473k respectively. At the inlet, all velocities of all phases were specified. At the outlet, the pressure was assumed to be Atmospheric pressure. The gas tangential normal velocities on the wall were set to zero (no slip condition). The following boundary equation was applied for the tangential velocity of Particle on the wall.

Boundary	**Condition**
Inlet1	Primary(Fluidized) Velocity inlet
Inlet2	Secondary Velocity inlet
Particle flow	Mass flow rate
Outlet	Pressure-outlet

XIII. NUMERICAL METHODOLOGY

A numerical method adopted to approximate the governing equations, along with the relevant boundary conditions, by a system of linear algebraic equations is known as a discretization method. Thus, a problem involving calculus is transformed into an algebraic problem which can then be solved on a computer by using a solution methodology. A discretization technique and a solution methodology constitute the numerical methodology used to solve a heat transfer and fluid flow problem. There are many discretization methods, but the most commonly used are the Finite difference method (FDM), the Finite volume method (FVM) and the Finite element method (FEM). During the early days of Computational fluid dynamics (CFD) finite-difference methods were the most popular. They are algorithmically simple, efficient, and accurate. However, they are best used on uniform grids and hence on regular computational domains. With advances of CFD, and its application to industrial problems, there is a need for methods for computing flows in complex geometries. To adapt the finite difference method to such geometries, we

can map the complex domain into simple domains, either globally or locally, and solve the equations there. However, such transformation makes the governing equations take quite complicated forms and may lead to a loss of computational efficiency and accuracy. Alternatively, one can use schemes based on the finite volume methods directly on the physical domain (i.e. without transformation).

Finite volume methods are essentially a generalization of the finite-difference method, but use the integral form of the governing equations of flow rather than their differential form. This gives greater flexibility in handling complex domains, as the finite volumes need not be regular. The FLUENT code, which is used to simulate the flow field is based on the finite volume discrtization scheme and is one of the best application software for this purpose.

XIV. RESULT AND DISCUSSION

XIV.I ANALYSIS OF COMBUSTION AT FLUIDIZING VELOCITY 4 m/s

TOTAL TEMPERATURE

When the fuel and air enter into the combustor, it burns due to high velocity and temperature and then temperature increase rapidly in the combustor. Finally obtained the result, the total temperature of the coal combustion is 1370(k).

The figure 4 shows that the temperature profile in circulating fluidized bed combustor. In this figure, the bed and temperature are increasing as soon as the coal particles are burning and finally obtained the maximum value of total temperature after coal combustion is 1370 K.

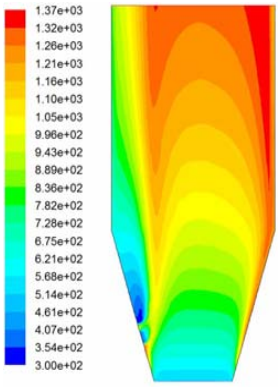

Fig.4 contours of total temperature (k)

Fig 5 shows the profile between the total temperature and the position of the combustor on all conditions such as default interior, pressure-outlet, primary air, secondary air and wall but fig.6 shows the plot the x-y diagram between total temperature and position of the combustor on pressure outlet condition.

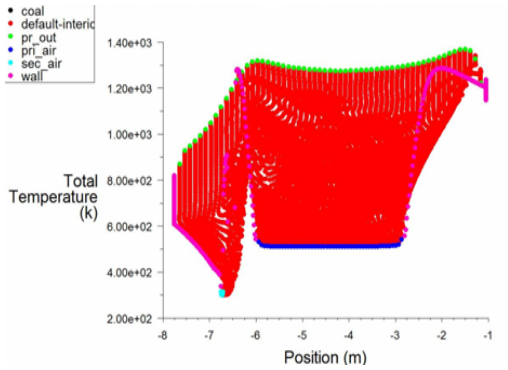

Fig.5. x-y plot of total temperature (k)

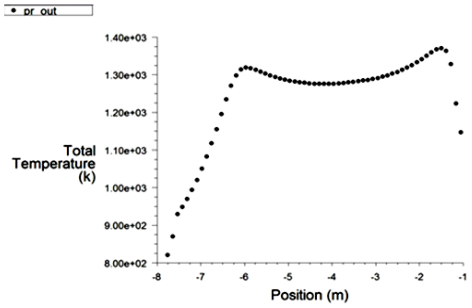

Fig.6 x-y plot of total temperature (k)

STATIC PRESSURE

The value of static pressure is found in the combustor is 5.63 (Pascal) after combustion process. The static pressure is rapidly increased when air fuel velocity enters in the combustion chamber. In the combustor, maximum static pressure is at the inlet points of the furnace.

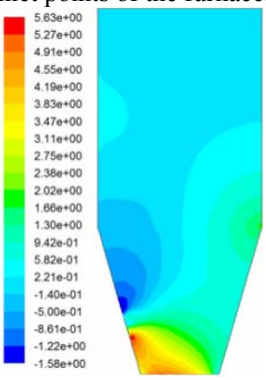

Fig.7 contours of static pressure (Pascal)

TURBULENCE KINETIC ENERGY

The maximum turbulence intensity is found to be $6.85e^{-01}$ after the combustion. In case of turbulence of kinetic energy, when the velocity of a gas is increased above the minimum bubbling velocity, the bed starts expanding. A continued increase in the velocity may eventually show a

change in the pattern of bed expansion. In the turbulent kinetic energy regime, the bubble phase loses its identity due to rapid coalescence and break up the bubbles. This results in a violently active and highly expanded bed with a change in the pattern of bed expansion.

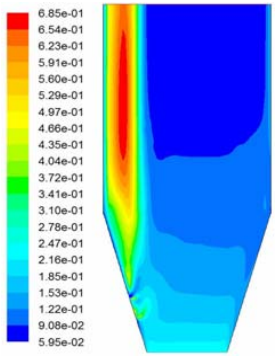

Fig.8 contours of turbulence kinetic energy (k) (m^2/s^2)

XIV.II ANALYSIS OF COMBUSTION AT FLUIDIZING VELOCITY 5m/s

TOTAL TEMPERATURE

The figure 40 shows that the temperature profile in circulating fluidized bed combustor. In this figure, the bed and temperature are increasing as soon as the coal particles are burning and finally obtained the maximum value of total temperature after coal combustion is 1372 k.

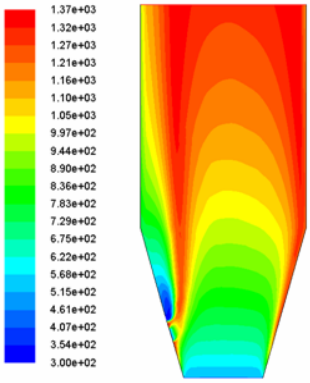

Fig.9 Contours of total temperature (k)

STATIC PRESSURE

The value of static pressure is found in the combustor is 8.01 (Pascal) after combustion process. The static pressure is rapidly increased when air fuel velocity enters in the combustion chamber. In the combustor, maximum static pressure is at the inlet points of the furnace.

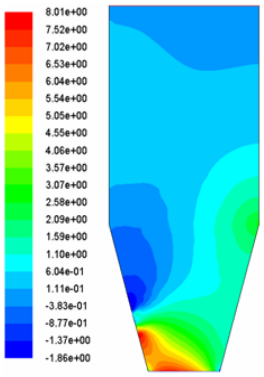

Fig.10 Contours of Static Pressure (Pascal)

TURBULENCE KINETIC ENERGY

The maximum turbulence intensity is found to be $6.85e^{-01}$ after the combustion. In case of turbulence of kinetic energy, when the velocity of a gas is increased above the minimum bubbling velocity, the bed starts expanding. A continued increase in the velocity may eventually show a change in the pattern of bed expansion. In the turbulent kinetic energy regime, the bubble phase loses its identity due to rapid coalescence and break up the bubbles. This results in a violently active and highly expanded bed with a change in the pattern of bed expansion.

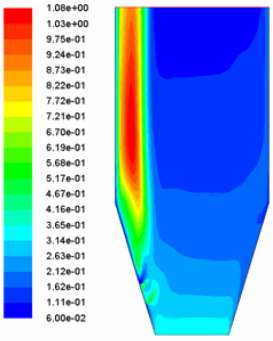

Fig.11 Contours of turbulence kinetic energy (k) (m^2/s^2)

XIV.III ANALYSIS OF COMBUSTION AT FLUIDIZING VELOCITY 6m/s

TOTAL TEMPERATURE

The figure 12 shows that the temperature profile in circulating fluidized bed combustor. In this diagram the bed and temperature are increasing as soon as the coal particles are burning and finally obtained the maximum value of total temperature after coal combustion is 1373 k.

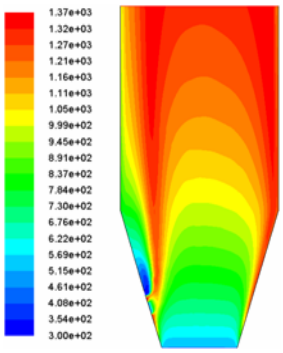

Fig.12 contours of total temperature (k)

STATIC PRESSURE

The value of static pressure is found in the combustor is 10.0 (Pascal) after combustion process. The static pressure is rapidly increased when air fuel velocity enters in the combustion chamber. In the combustor, maximum static pressure is at the inlet points of the furnace.

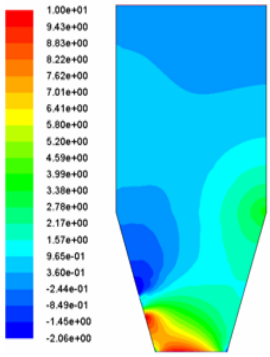

Fig.13 Contours of static pressure (Pascal)

TURBULENCE KINETIC ENERGY

The maximum turbulence intensity is found to be 1.43 after the combustion. In case of turbulence of kinetic energy, when the velocity of a gas is increased above the minimum bubbling velocity, the bed starts expanding. A continued increase in the velocity may eventually show a change in the pattern of bed expansion. In the turbulent kinetic energy regime, the bubble phase loses its identity due to rapid coalescence and break up the bubbles. This results in a violently active and highly expanded bed with a change in the pattern of bed expansion

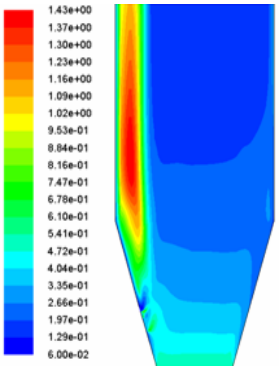

Fig.14 Contours of turbulence kinetic energy (k) (m2/s2)

XV. BEHAVOIUR OF TOTAL TEMPERATURE AT DIFFERENT FLUIDIZING VELOCITIES

Following are the trends of Total temperature vs. inlet air velocity obtained at different inlet fluidizing velocities, which show that temperature increases when air velocity is increased.

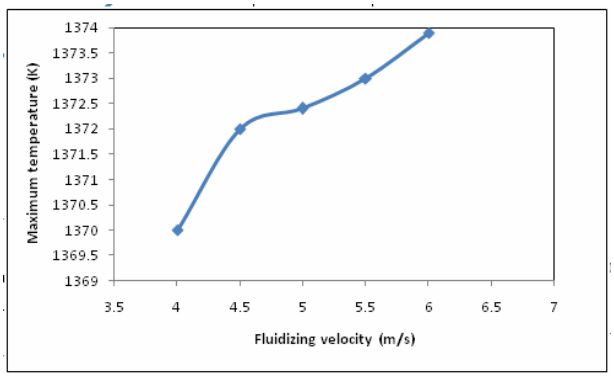

Fig.15 Temperature versus different fluidizing velocity

XVI. BEHAVIOUR OF PRESSURE AT DIFFERENT FLUIDIZING VELOCITIES

Following plots of various pressures vs. inlet air velocity obtained at different fluidizing velocities. This plots show that pressure increases as air velocity is increased. This is because with increase in air velocity and mass flow rate of fuel in the combustor increases thereby increasing the pressure across the combustor. In this fig.16,when the fluidizing velocity is 4m/s at the inlet of combustor then the static pressure is observed 5.63 Pascal after coal combustion in the combustor of CFB i.e. the static pressure is increases with increasing the inlet velocity. The same conditions are for total and dynamic pressure.

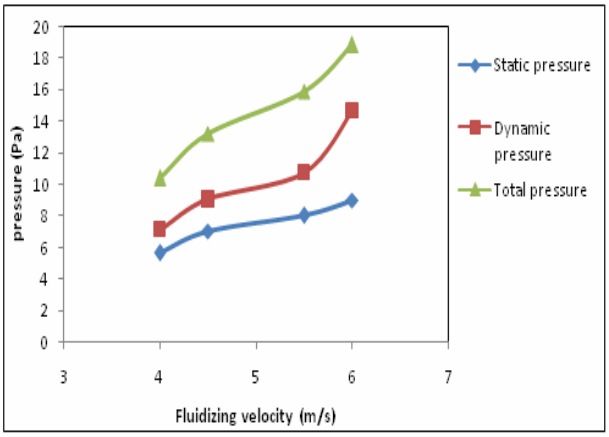

Fig.16 Pressures versus different fluidizing velocity.

XVIII. CONCLUSION

In this work, analysis of coal combustion in circulating fluidized bed has been performed at three different fluidizing velocities with fluent software.
Following conclusions are drawn from the computational analysis in this present work.
The following conclusions are:

1) It is observed that the change in maximum total temperature for the three fluidizing velocities i.e. 4m/s, 5m/s and 6m/s is insignificant.

2) Maximum static pressure increases from 5.63Pa to 10Pa, when fluidizing velocity is increased from 4m/s to 6m/s. This increase in the static pressure inside the combustion chamber is because there is no leakage of air from the combustion chamber.

3) Maximum total pressure increases from 10.4 Pa to 22 Pa, when fluidizing velocity is increased from 4m/s to 6m/s. Maximum total pressure values are more than maximum static pressure values at the same fluidizing velocity as it includes dynamic pressure also.

4) The maximum turbulent intensity of the mixture increases from 67.6% to 97.8%, when fluidizing velocity is increased from 4m/s to 6m/s.

5) In fluidized bed combustion, a number of parameters are important such as temperature, pressure, as it has been observed that all the parameters temperature and pressure are better for combustion at fluidizing velocity 6m/s. Therefore, a fluidizing velocity of 6m/s is suitable for fluidized bed combustion as compared to 4m/s and 5m/s.

XVII. GRID INDEPENDENCE TEST

The resolution of the grid has a great quantitative impact over the results obtained. There exists a level of refining of a computational domain beyond which there is no significant quantitative changes in the results achieved. The computational domain at this level of refinement is said to enter the regime of grid independence.
The temperature variation along the combustor is studied for these levels of refinement. The results are compared and the computational grid structure with the level of refining from which no change in the temperature variation along the combustor is seen with further refinement, is chosen for detailed analysis. This particular grid is said to undergo grid independence test.

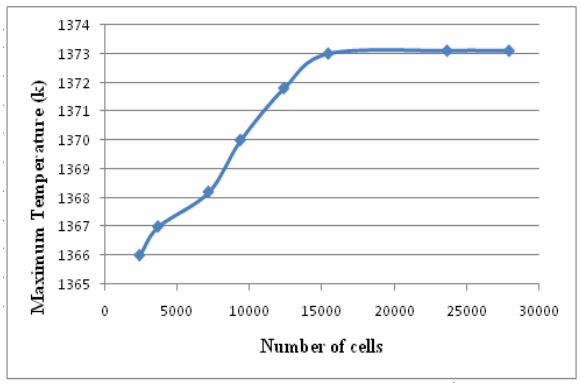

Fig 17: Plot temperature profile vs. number of cells

To find out the most independent grid for CFD analysis of model of CFB combustor, grid independency of the solution was established. Based on the different grids, analysis have been made and it was observed that after refining the grid from cells 15435, results are not varying significantly. So, cells15435 have been used for further analysis.

Notation

ρ = Density
$\vec{V}$ = Velocity vector
p = Static pressure
$\bar{\bar{\tau}}$ = Stress tensor
$\rho\vec{g}$ = Gravitational body force
P= Pressure
μeff= Effective viscosity
K= Turbulent kinetic energy
ε= Dissipation rate of turbulent kinetic energy
T= Temperature
g= Acceleration due to gravity
k_{eff} = Effective conductivity
k_t = Turbulent thermal conductivity
μ = molecular viscosity
I = unit tensor
h – Sensible enthalpy

REFERENCES

[1] Martin Junginger, Development of fluidized bed combustion—An overview of trends, performance and cost. Progress in Energy and Combustion Science 2007; 33: 19–55.

[2] A. Williams and M. Pourkashanian, The Combustion of Coal and Some Other Solid Fuels.2000; 28: 2141–2162.

[3] Konstantin P. Filipov ,Numerical Modeling Of Coal Combustion Processes In Ecological Clear Circulating Fluidized Bed Boiler Units, Novosibirsk State Technical University 630092.

[4] Z.Guangbo, A coal combustion model for circulating fluidized bed boilers. Fuel 2000; 79: 165–172.

[5] Afsin Gungor, Hydrodynamic modeling of a circulating fluidized bed, Powder Technology 2007; 172: 1–13,

[6] Hideya Nakamura, Numerical modeling of particle fluidization behavior in a rotating fluidized bed, Powder Technology 2007; 171: 106–117.

[7] Aboozar Hadavand, An innovative bed temperature-oriented modeling and robust control of a circulating fluidized bed combustor, Chemical Engineering Journal 2008; 140: 497–508.

[8] L.X. Kong and P.D. Hodgson, Computational simulation of gas flow and heat transfer near an immersed object in fluidized beds, Advances in Engineering Software 2007;38: 826–834.

[9] J.C.S.C. Bastos, Modelling and simulation of a gas–solids dispersion flow in a high flux circulating fluidized bed (HFCFB) riser, Catalysis Today 2008; 130: 462–470.

[10] I. Petersen and J.Werther, Three-dimensional modeling of a circulating fluidized bed gasifier for sewage sludge. Chemical Engineering Science 2005; 60: 4469–4484.

[11] Vidyasagar Shilapuram, Comparison of macroscopic flow properties obtained by three methods of operation in a liquid–solid circulating fluidized bed, Chemical Engineering and Processing 2009;48: 259–267.

[12] Jack T.Cornelissen, CFD modelling of a liquid–solid fluidized bed, Chemical Engineering Science 2007; 62:6334 – 6348.

[13] Xiao-Bo Qi, Friction between gas–solid flow and circulating fluidized bed downer wall, Chemical Engineering Journal 2008;142: 318–326.

[14] Haiyan Zhu, Detailed measurements of flow structure inside a dense gas–solids fluidized bed, Powder Technology 2008; 180: 339–349.

[15] Zhongxiang Chen, Comparison of fluidized bed flow regimes for steam methane reforming in membrane reactors: A simulation study. Chemical Engineering Science 2009; 64: 3598 – 3613.

[16] Stephen J. Goidich, Foster Wheeler Compact CFB Boilers for Utility Scale, Foster Wheeler Energy International, Perryville Corporate Park Clinton, New Jersey, USA 08809-4000.

[17] Adnan Almuttahar, Computational fluid dynamics of high density circulating fluidized bed riser: Study of modeling parameters. Powder Technology 2008; 185:11–23.

[18] Ernst-Ulrich Hartge, CFD-simulation of a circulating fluidized bed riser, Particuology 2009; 7: 283–296.

[19] Xiao-Bo Qi and Hui Zhang, Solids concentration in the fully developed region of circulating fluidized bed downers, Powder Technology 2008;183: 417–425.

[20] Jinsen Gao and Jian Chang, Experimental and computational studies on flow behavior of gas–solid fluidized bed with disparately sized binary particles, Particuology 2008; 6: 59–71.

[21] Ernst-Ulrich Hartge, CFD-simulation of a circulating fluidized bed riser, Particuology 2009; 7: 283–296.

[22] Filip Johnsson, Macroscopic modelling of fluid dynamics in large-scale circulating fluidized beds, Progress in Energy and Combustion Science 2006; 32: 539–569.

[23] Dongsheng Wen and Yurong He, Modelling of the behaviour of gas–solid two-phase mixtures flowing through packed beds, Chemical Engineering Science 2006; 61:1922 – 1931.

[24] Peng Li, Drag models for simulating gas–solid flow in the turbulent fluidization of FCC particles, Particuology 2009; 7: 269–277.

[25] Nan Zhang, Virtual experimentation through 3D full-loop simulation of a circulating fluidized bed. Particuology 2008; 6: 529–539.

[26] Ranjeet P. Utikar, Single jet fluidized beds: Experiments and CFD simulations with glass and polypropylene particles, Chemical Engineering Science 2007; 62: 167 – 183.

[27] Scott Cooper, CFD simulations of particle mixing in a binary fluidized bed. Powder Technology 2005; 151: 27– 36.

[28] Fluent User Guide, Fluent Inc. January 11, 2005.

[29] Kari Myöhänen and Vesa Tanskanen, CFD Modelling Of Fluidized Bed Systems,Lappeenranta University of Technology, FI-53851 Lappeenranta, Finland.